Acta Applicandae Mathematicae (2005) 87: 281–307
DOI: 10.1007/s10440-005-1164-7

Interpretation of Quantum Hamiltonian Monodromy in Terms of Lattice Defects

B. ZHILINSKII
Université du Littoral, UMR du CNRS 8101, 59140 Dunkerque, France.
e-mail: zhilin@univ-littoral.fr

Abstract. The analogy between monodromy in dynamical (Hamiltonian) systems and defect in crystal lattices is used in order to formulate some general conjectures about possible types of qualitative features of quantum systems which can be interpreted as a manifestation of classical monodromy in quantum finite particle (molecular) problems.

Mathematics Subject Classifications (2000): 37J05, 70H33, 81Q70.

Key words: monodromy, defects, molecules.

1. Introduction

The purpose of this paper is to demonstrate amazing similarity between apparently different subjects: defects of regular periodic lattices, monodromy of classical Hamiltonian integrable dynamical systems, and qualitative features of joint quantum spectra of several commuting observables for quantum finite-particle systems.

The physical motivation comes from the qualitative analysis of quantum finite particle systems (molecules). Many important features of the system of quantum eigenstates can be understood if one finds a physically reasonable system of approximate "good quantum numbers" or equivalently a set of mutually commuting operators. In the classical limit such approximate models correspond to integrable models which nevertheless can possess nontrivial qualitative features like Hamiltonian monodromy. Monodromy, which is the topological obstruction to the existence of global action-angle variables, naturally, manifests itself in the joint spectrum of mutually commuting quantum operators. Thus it is important to find the correspondence between typical singularities which are present for classical integrable models and specific patterns in the joint spectra of corresponding commuting observables for associated quantum problems. In the case of a regular classical integrable fibration, the joint spectrum of the corresponding quantum observables can be represented as a system of points labeled by quantum numbers $(n_1, \dots, n_k)$ taking integer values. They form regular lattice of quantum states which can be interpreted as a part of a standard k-dimensional lattice, Z^k. In a more general case of quantum problems which in the classical limit lead to integrable fibrations with singularities the joint spectrum can be mapped on Z^k lattice only locally. Globally, it can be described as a lattice with defects. Following the general idea of solid state physics to describe different defects as a result of "cutting and gluing" of an "ideal" lattice we apply the same construction to the "quantum state lattice" which represents the joint spectrum of a set of mutually commuting operators.

First of all we describe several "elementary monodromy" defects which appear naturally in the qualitative description of "quantum state lattices". Starting with integer monodromy defects we generalize them to fractional monodromy defects and describe their relation with associated singularities of classical integrable systems. Finally we suggest several examples of molecular quantum systems which show different types of quantum monodromy and lattice defects.

2. Elementary Monodromy Defect in 2D-Lattice

Let us start with the regular two-dimensional (2D)-lattice L which will be used below to construct more complicated objects, namely lattices with defects. Each vertex of the lattice L is labeled by two integers in such a way that there is an isomorphism between L and the lattice Z^2 of integer numbers. To represent the lattice we use the Cartesian coordinate system on the plane $R^2 = \{x, y\}$ and take as vertices all points with integer coordinates (n_x, n_y). We will choose as an "initial" elementary cell of the lattice the cell formed by four vertices labeled by (n_x, n_y), $(n_x + 1, n_y)$, $(n_x, n_y + 1)$, $(n_x + 1, n_y + 1)$. The vertex (n_x, n_y) will be referred as the origin of the cell. Two oriented sides which begin at the (n_x, n_y) vertex and end at $(n_x + 1, n_y)$ and $(n_x, n_y + 1)$ vertices form the frame of the cell. We write the frame in the form of 2×2 matrix whose first (second) column is given by the projection of the first (second) side of the cell on x and y axes.

Such a choice of an elementary cell is not unique. The lattice is invariant with respect to any transformation from the group GL(2, Z) of 2×2 matrices with integer coefficients and with determinant ± 1. At the same time when we establish a correspondence between abstract lattice Z^2 and concrete physical problem with two commuting observables the choice of variables should be fixed. Below we suppose that the choice of basis has specific physical meaning and is held fixed.

As soon as the initial elementary cell is chosen we can transport it through the lattice by making elementary steps in x or in y directions. Each elementary step consists in moving the origin of the cell by changing the n_x (or n_y) integer by one for all four vertices of the cell. Naturally for a regular lattice we can transport the elementary cell with given origin (n_x, n_y) to the cell having origin at any other vertex (n'_x, n'_y). The frame is transformed in such a case by a parallel transport over the lattice.

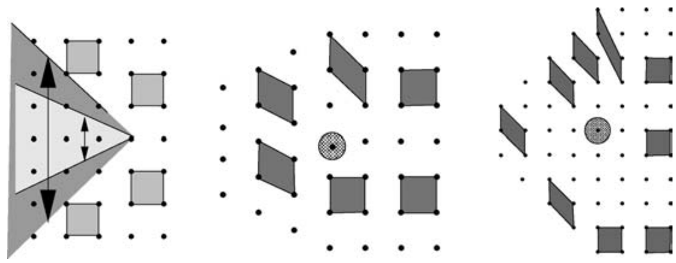

Figure 1. Construction of the monodromy defect by removing one of the solid angles (bounded by $2|y| = -x$ and $|y| = -x$ rays) shown on the left picture. Reconstructed lattices after removing small or large sectors are shown together with transport of elementary cell along a closed path around the defect on the reconstructed lattice. The identification of boundaries after removing solid angle is done by the parallel shift of lattice points in vertical direction.

Starting from the regular Z^2 lattice in R^2 we construct a lattice with "elementary monodromy defect" by performing the following two steps:

(i) We remove part of the lattice by doing special cuts;
(ii) We define "matching rules" which specify how to cross the cut, i.e. how to transport the cell over the removed part of the lattice.

To be more precise, let us consider the set $\mathcal{C}(x:y) = \{(x, y) \in R^2 \mid x < -2|y|\}$ which we call a wedge (see Figure 1, left). We remove the wedge from the lattice and identify the points $(n_x = -2n, n_y = n) = (n_x = -2n, n_y = -n)$ for every positive integer n. In other words, we glue the two boundaries of the wedge by parallel transport of points on the boundary in vertical direction. We can imagine the result of this "cut and glue" construction as a lattice with a point defect, see Figure 1, center and right.

We call the constructed object the lattice with an "elementary monodromy defect". The origin of the removed wedge is a defect point. The reason for this nomenclature follows from the rules of the transportation of the elementary cell along a closed path in the lattice with defect. If the closed path does not surround the defect point the transportation of an elementary cell along such path does not modify the cell even if the path crosses the cut several (even number of) times. At the same time the elementary cell changes its form after transportation along a closed path which surrounds the defect point and crosses the cut once.

When the elementary cell crosses the cut the sides of the cell which are orthogonal to the cut (angle-bisector of the removed wedge) remain unchanged. At the same time other sides change their slope with respect to x axis. After a round trip encircling the defect point the elementary cell changes its form while its volume remains constant. Each elementary cell defines a frame. We express the transformation between two frames with the same origin in a matrix form. The matrix transforming initial frame into final one (obtained after a closed trip of the cell around the defect) is called the quantum monodromy matrix. Each column of this matrix gives the expression of new sides of the final elementary cell in terms of the sides of the initial cell. For example, the matrix corresponding to transformation of the elementary cell in the clockwise direction shown in Figure 1 has the form $\begin{pmatrix} 1 & 0 \\ -p & 1 \end{pmatrix}$, where $p = 1$ (2) corresponds to case where a small (large) wedge is removed from the initial regular lattice. The sign of the nondiagonal element depends on the direction in which the cut is crossed. The form of the matrix in general depends naturally on the choice of the cut and on the choice of the cell. If the basis is not specified the quantum monodromy matrix is defined up to similarity transformation with arbitrary SL(2, Z) matrix.

The simplest modification of the cut consists in its realization along axis y instead of axis x. In such a case the identification of points on the boundaries should be done by sliding the vertices of each row parallel to axis x.

Figure 2 shows an example of regular lattice with four elementary monodromy cuts. Two cuts along x axis are made in different directions. The other two are made along y axis again in different directions. The initial elementary cell is chosen in the left lower corner and is moved along a path in the counterclockwise direction which consecutively crosses all four cuts and surrounds four elementary defects. The frame associated to the elementary cell is defined by two sides of the cell, namely Oa and Ob. The first and the second columns of the matrix characterizing the frame give expressions of the side Oa and of the side Ob in

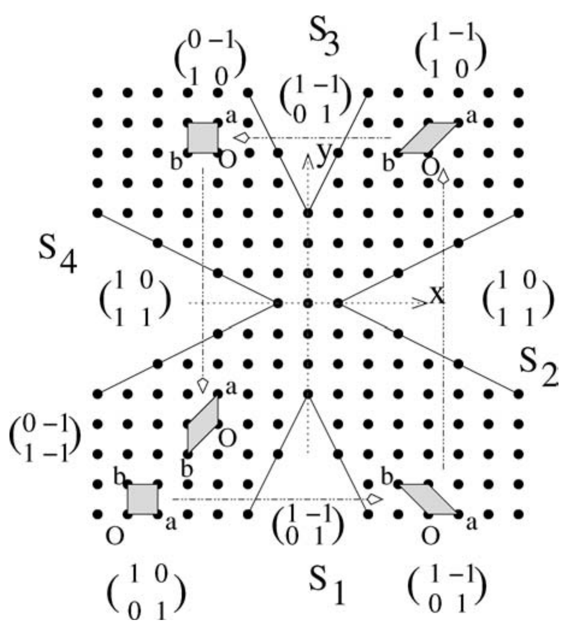

Figure 2. Example of regular lattice with four cuts. Evolution of the elementary cell along the path crossing all cuts is shown together with matrices defining the frame in $\{x, y\}$ basis and matrices corresponding to crossing each elementary cut.

term of the chosen initial frame. The matrices M_i describing transformation of elementary cell crossing each of the cuts, S_i, in the counterclockwise direction have the form $M_1 = M_3 = \begin{pmatrix} 1 & -1 \\ 0 & 1 \end{pmatrix}$, $M_2 = M_4 = \begin{pmatrix} 1 & 0 \\ 1 & 1 \end{pmatrix}$, see Figure 2. These matrices coincide with the quantum monodromy matrices for corresponding isolated defects supposing that the defect is surrounded by the counterclockwise path. If the direction of the path is reversed the inverse of the matrix should be taken. Note that matrices for S_1 and S_3 cuts, as well as for S_2 and S_4 cuts, are the same. In order to find the matrix corresponding to modification of the cell along a path crossing consecutively several cuts it suffices to left-multiply matrices for individual cuts. For example, the matrix M corresponding to path in Figure 2 surrounding all four defects in the counterclockwise direction has the form

$$\begin{aligned} M = M_4 M_3 M_2 M_1 &= \begin{pmatrix} 1 & 0 \\ 1 & 1 \end{pmatrix} \begin{pmatrix} 1 & -1 \\ 0 & 1 \end{pmatrix} \begin{pmatrix} 1 & 0 \\ 1 & 1 \end{pmatrix} \begin{pmatrix} 1 & -1 \\ 0 & 1 \end{pmatrix} \\ &= \begin{pmatrix} 0 & -1 \\ 1 & -1 \end{pmatrix}. \end{aligned} \tag{1}$$

Going along the same closed path in the reverse direction leads to inverse transformation $M^{-1} = M_1^{-1} M_2^{-1} M_3^{-1} M_4^{-1}$.

2.1. ORIENTATION OF CUTS

We can formally define the "elementary monodromy defect" by cutting the regular square lattice in a less symmetrical way. This means that the two boundary rays of a wedge can be placed more or less arbitrarily but the system of axes and rules for identification of boundary points remain the same. The only real restriction is the conservation of the number of removed points from each column. Figure 3 shows three different choices of removed wedges which result in the point defect with the same monodromy matrix after the identification or two boundaries through the vertical displacement. This shows that the construction of the defect by making the

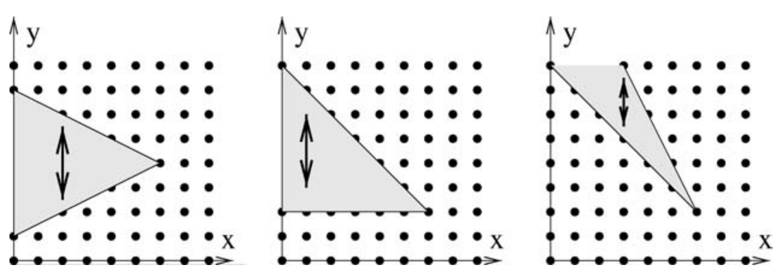

Figure 3. Three choices of removed slices resulting in the point defect with the same monodromy. The number of points removed from any $x = \text{const}$ column is the same for all three examples.

cut explicitly is an auxiliary tool and the details of the geometry of the cut are not important.

At the same time the choice of basis of the lattice is important for the construction of the defect. If we change the initially fixed x, y axes to SL(2, Z) equivalent directions and repeat the construction of the lattice with elementary defect which has the same monodromy matrix M in the new system of axes, we obtain an SL(2, Z) equivalent defect. The monodromy matrix for this defect with respect to the initial basis has the form AMA^{-1} with $A \in$ SL(2, Z). Let us note that the two "elementary defects" introduced in the beginning as the result of a cut along x and along y directions are unimodular equivalent. To see this we just need to introduce the SL(2, Z) matrix which changes x into y and y into $-x$, i.e. $V = \begin{pmatrix} 0 & -1 \\ 1 & 0 \end{pmatrix}$. The similarity transformation of the monodromy matrix $M = \begin{pmatrix} 1 & 0 \\ 1 & 1 \end{pmatrix}$, associated with the "elementary monodromy defect" constructed through the cut along the x direction is

$$VMV^{-1} = \begin{pmatrix} 0 & -1 \\ 1 & 0 \end{pmatrix} \begin{pmatrix} 1 & 0 \\ 1 & 1 \end{pmatrix} \begin{pmatrix} 0 & 1 \\ -1 & 0 \end{pmatrix} = \begin{pmatrix} 1 & -1 \\ 0 & 1 \end{pmatrix}, \tag{2}$$

which corresponds to the "elementary monodromy defect" constructed in the same lattice basis using a cut along the y direction (see Figure 2).

In the case of presence of only one defect within the regular lattice the ambiguity of the choice of lattice basis is unimportant. It is interesting to note that two defects in the same lattice basis characterized by monodromy matrices $M = \begin{pmatrix} 1 & 0 \\ \pm 1 & 1 \end{pmatrix}$ with different sign of nondiagonal element should be considered as different because these matrices are not conjugate in SL(2, Z).

Later in physical applications related with integrable dynamical systems we will study lattices of quantum states which are bounded in some directions. This means that the boundary imposes a particular choice of the lattice basis and of elementary cell in the sense that different choices can be distinguished by their orientation with respect to boundaries.

2.2. SIGN OF THE DEFECT

Another way to generalize the construction of the elementary monodromy defect is to incorporate the wedge into lattice after making a cut of a regular lattice rather than removing it from the lattice. In order to distinguish between defects obtained by removing and adding wedges we will denote defects obtained by removing wedge from the lattice (as was explained at the beginning of this section) by the sign $-$, namely ${}^{(-)}S$, and defects obtained by adding wedge by sign $+$, namely ${}^{(+)}S$. For reasons related to dynamical interpretation of defects we assume that the sign of a defect is negative if the contrary is not specified explicitly.

The simplest construction of a positive elementary monodromy defect consists in

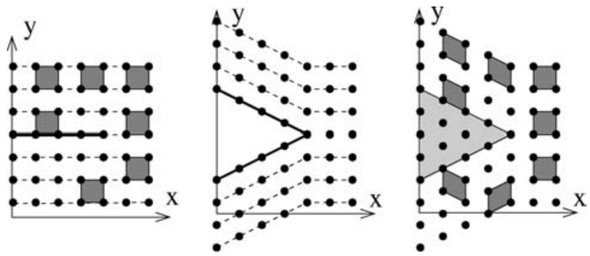

Figure 4. Construction of the positive “elementary monodromy defect”.

(i) making a cut parallel to the x axis starting at vertex O;
(ii) opening the cut by sliding vertices in vertical direction;
(iii) introducing a wedge of regular lattice into the cut.

This procedure is illustrated in Figure 4.

2.3. CHARACTERIZATION OF A DEFECT

Now we summarize the characteristics of “elementary monodromy defects” which follow from the method of cutting and gluing a regular lattice.

(i) “Sign” of the defect, which specifies the decrease or increase of the number of vertices in the lattice after the “cut and glue” procedure.
(ii) “Amplitude”, p, of the defect which can take any positive integer value.
(iii) “Orientation” of the defect, given by the unimodular matrix, which specifies the lattice basis in which the cutting and matching rules defining the defect are realized.

The sign and the amplitude are basis independent characteristics of “elementary defects”.

Below we suppose that the basis is fixed and use the following notation.

An elementary negative cut in x direction with amplitude $p = 1$ is denoted by ${}^{(-)}S_v^1$. The lattice obtained after making this cut is constructed by identifying points on the cut boundary by a vertical displacement. An elementary negative cut in y direction with amplitude $p = 1$ is denoted by ${}^{(-)}S_h^1$. The lattice obtained after making this cut is reconstructed by identifying points on the cut boundary by a horizontal displacement.

When the amplitude, p, of the elementary defect is larger than 1, we call such defect multiple. All defects which in some lattice basis can be represented by one negative or one positive (multiple) cut will be considered to be elementary. Monodromy matrices for such cuts belong to classes of conjugate elements of SL(2, Z) group represented by matrices $\begin{pmatrix} 1 & 0 \\ p & 1 \end{pmatrix}$ with p being an integer. The converse statement is not true. There exist nonelementary cuts (or systems of cuts) such that their monodromy matrices coincide with monodromy matrices for some elementary cuts. To see this we need to look a little more at nonelementary defects.

2.4. NONELEMENTARY DEFECTS

Let now suppose that regular lattice has several elementary defects, $S_1, S_2, \ldots$, realized with different choices of lattice basis and elementary cells. This means that monodromy matrices for each elementary defect can be transformed by a similarity SL(2, Z) transformation to the particular simple form $M_i = \left(\begin{smallmatrix} 1 & 0 \\ p_i & 1 \end{smallmatrix}\right)$. With respect to the initial basis of the regular lattice the monodromy matrices have the form $A_i M_i A_i^{-1}$ with $A_i \in$ SL(2, Z). If one takes now the loop which goes around several elementary defects the resulting monodromy matrix has the form of a product $\prod_i A_i M_i A_i^{-1}$. It is known that arbitrary SL(2, Z) matrix can be represented as such a product (see [25, 8, 9]). Consequently, by collecting the vertices of several elementary cuts into one point we can construct a nonelementary defect with arbitrary SL(2, Z) monodromy matrix.

It is interesting to note that in order to construct a nonelementary point defect with any given monodromy matrix we can use only defects of the same sign done in some chosen basis only along x and along y axes. This is a direct consequence of an elementary property of SL(2, Z) group:

THEOREM ([25], Theorem 1.2.4). *As a group* SL(2, Z) *is generated by two elements* $U = \left(\begin{smallmatrix} 1 & 1 \\ 0 & 1 \end{smallmatrix}\right)$ *and* $V = \left(\begin{smallmatrix} 0 & -1 \\ 1 & 0 \end{smallmatrix}\right)$. *In other words, every element* $T \in$ SL(2, Z) *can be written in the form* $T = U^{q_0} V U^{q_1} \cdots V U^{q_n}$, *where* $q_i \in Z$ $(0 \leqslant i \leqslant n)$. *This representation is not unique.*

To deduce from this theorem the possibility to construct defects with arbitrary monodromy by doing only simple cuts along x and y axes it is sufficient to show that V can be constructed from three such elementary defects [33], namely:

$$\begin{pmatrix} 0 & -1 \\ 1 & 0 \end{pmatrix} = \begin{pmatrix} 1 & -1 \\ 0 & 1 \end{pmatrix} \begin{pmatrix} 1 & 0 \\ 1 & 1 \end{pmatrix} \begin{pmatrix} 1 & -1 \\ 0 & 1 \end{pmatrix}. \tag{3}$$

In Figure 5 we give an example suggested by V. Matveev (private communication) of a lattice with 11 elementary negative defects chosen in such a way that their global effect is equivalent to a positive elementary monodromy defect. Using the notation ${}^{(-)}S_v^p$, ${}^{(-)}S_h^p$ for elementary defects, the nonelementary system of cuts represented in Figure 5 forms the following sequence when going in the counterclockwise direction starting from the right lower corner:

$${}^{(-)}S_v^2,\ {}^{(-)}S_h^1,\ {}^{(-)}S_v^2,\ {}^{(-)}S_h^1,\ {}^{(-)}S_v^2,\ {}^{(-)}S_h^1,\ {}^{(-)}S_v^2.$$

The global monodromy matrix of such a system of elementary defects gives the same monodromy matrix as the elementary positive defect ${}^{(+)}S_h^1$. To see this geometrically it is sufficient to compare initial and final cells shown in Figure 5.

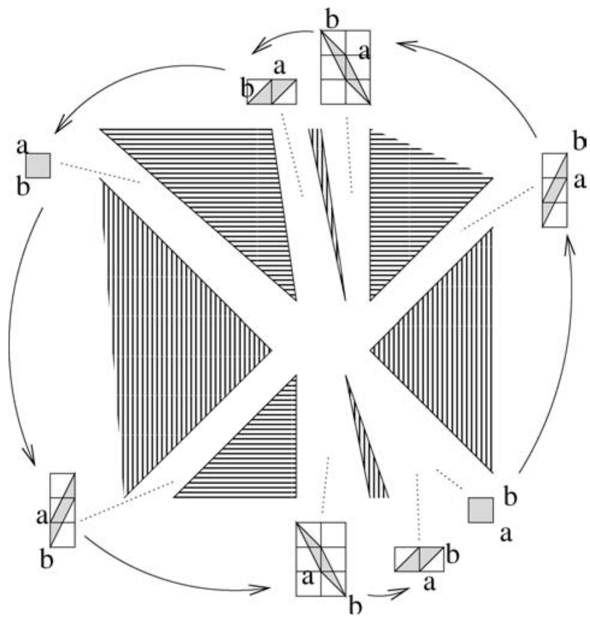

Figure 5. Lattice with 11 elementary negative monodromy defects. Wedges with vertical (horizontal) hatching correspond to removed parts of the lattice with identification of boundaries by vertical (horizontal) displacements. Transformation of the elementary cell after crossing each cut is shown around the figure.

The fact that only elementary defects of one (negative or positive) sign are sufficient to construct nonelementary defects with arbitrary monodromy matrix shows that the monodromy matrix is not sufficient to distinguish between different defects. The sign is an important characteristic of a defect. Moreover, the representation of the identity monodromy matrix as a result of 12 elementary monodromy defects of the same sign clearly shows that there are qualitatively different systems of defects which have the same global monodromy matrix [8, 9].

3. Fractional Monodromy Defect in 2D-Lattice

The principal point in constructing a defect by cutting out a wedge of the lattice is the proper choice of the wedge. In the discussed above construction of the elementary defects the number of points removed from each column is the linear function of the column number which takes integer values. In such a case the resulting point defect is characterized by the monodromy matrix with integer coefficients.

Now we generalize this construction [33, 32]. We do a rational cut. This means that starting from some point of Z^2 lattice we make a cut with straight boundaries in such a way that we remove m points from the nth column. We assume that m/n is a rational number. In other words, the number of removed points from

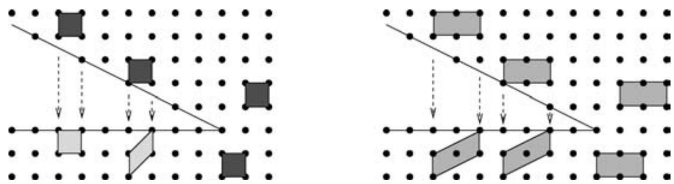

Figure 6. Construction of the 1 : 2 rational lattice defect starting from the regular square lattice. (Left) – Ambiguity in the transfer of 1 × 1 cell through the cut. (Right) – Unambiguous transfer of double cell through the cut.

column is assumed to be a linear function with periodic coefficients. Such objects are known as quasi-polynomials [29]. Their application to the description of the density of quantum states via the generating function formalism is briefly reviewed in [26, 21, 31]. Due to oscillatory contribution to the number of removed states the lattice constructed after such cut by identifying points on the boundary of the cut by parallel gliding possesses line defect rather than the point defect.

The simplest example of such construction, namely 1 : 2 cut, is shown in Figure 6.

In order to interpret the 1 : 2 rational cut it is useful to consider two sub-lattices of index 2 instead of the initial lattice. Each of these sub-lattices has elementary monodromy cut of the 1 : 1 type. In another words the transformation of the elementary cell for each sub-lattice clearly shows the presence of elementary monodromy defect for this sub-lattice. Written in terms of the initial lattice the monodromy becomes fractional.

Again, as in the case of integer monodromy, the geometrical construction of the removed wedge is ambiguous. There are more serious restrictions in the case of fractional defect than in the case of integer elementary monodromy defect.

In the case of integer monodromy defect we remove from each "vertical line" an integer number of points. These points are situated on the closed interval which is a multiple of a side of elementary cell. Two end points of the removed interval should be identified in order to reconstruct the lattice after cutting a wedge. Thus the number of removed points from each vertical line of the lattice is always equal the length of the interval. In the case of a fractional cut the removed interval is not an integer multiple of the distance between vertices. Consequently the number of points on the removed interval changes if we simply move interval along the transportation line through the cut.

Figure 7 shows the construction of 2 : 3 rational cut by making initial arbitrary cut with respect to the lattice basis. Let us suppose that this cut corresponds to the lower boundary of the removed wedge and its slope with respect to the x axis is $\tan\alpha$. In order to find the upper boundary we need to draw a line which has slope $\tan\beta = \tan\alpha + 2/3$. Although such construction seems to be similar to the construction of the integer cut there is important difference. The oscillatory contribution to the number of removed points from each vertical line depends

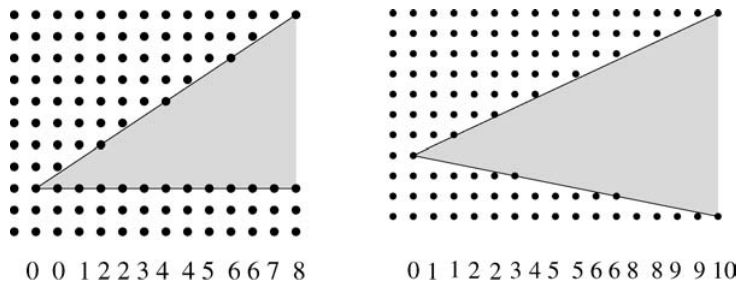

Figure 7. Construction of the 2 : 3 rational lattice defect by cutting out two different wedges from the regular square lattice. (Left) – Each boundary of the cut is done through the vertices which belong to the sub-lattice compatible with the 2 : 3 defect. (Right) – The boundary of the cut belongs to the sub-lattice with index multiple to 5 which is not compatible with the 2 : 3 defect of the initial lattice. The numbers of removed states from each column is shown in both cases.

on $\tan\alpha$. Figure 7 illustrate this effect. In order to fix the oscillatory contribution the cut should be done through vertices which belong to sub-lattice in which the represented cut becomes an integer cut. Naturally for such sub-lattice the position of the cut can vary in the same way as for integer monodromy defect.

4. Defects in 3D-Lattice

Let us now generalize the construction of defects from 2D-lattice to 3D-lattice. We start again with integer defect. The trivial extension of the removed 2D-solid angle to 3D-solid angle leads after reconstruction of the 3D-lattice to 1D-line defect. The same trivial generalization of the point defect for 2D-lattice to N-dimensional lattice results in the $(N-2)$-dimensional defect, i.e. the codimension 2 defect. In order to characterize the line defect of a 3D-lattice obtained by removing a 3D-solid angle in terms of cell transformation in a way similar to the cell transformation for 2D-lattices with defects, we need to choose the 3D-elementary cell and to study its evolution along the closed path surrounding the line defect.

Although the extension of the construction to 3D-lattice is in some sense trivial there are some interesting new features. First of all we immediately note that the sign of the monodromy matrix characterizing the elementary defect is not well defined (in contrast to 2D-case). This means that by modification of the choice of elementary cell by a similarity transformation with SL$(3, Z)$ matrix we can change the sign of nondiagonal element of the monodromy matrix. Figure 8 illustrates this. It shows two alternative choices of the 3D-cell given by frames $\{e_1, e_2, e_3\}$ and $\{f_1, f_2, f_3\}$. These two frames are related by transformation which belongs to SL$(3, Z)$ group:

$$\begin{pmatrix} f_1 \\ f_2 \\ f_3 \end{pmatrix} = \begin{pmatrix} 1 & 0 & 0 \\ 0 & -1 & 0 \\ 0 & 0 & -1 \end{pmatrix} \begin{pmatrix} e_1 \\ e_2 \\ e_3 \end{pmatrix}. \tag{4}$$

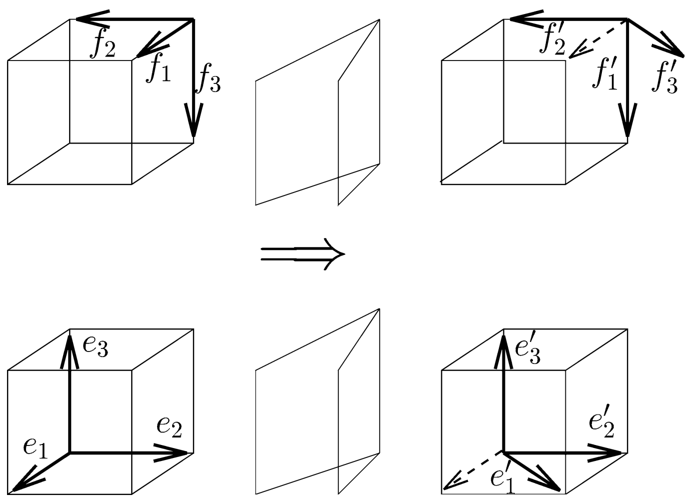

Figure 8. Transformation of the elementary 3D-cell after going through the negative elementary monodromy cut of the 3D-lattice. Two different choices of frames are shown: $\{e_1, e_2, e_3\}$ and $\{f_1, f_2, f_3\}$, which differ one from another by a proper orthogonal SL(3, Z) transformation (rotation over π around e_1).

Transformation of each frame when going through the elementary cut (associated with the removed wedge) coincides with the monodromy matrix of the cell corresponding to closed path around the negative defect line constructed by removing the 3D-wedge. In the two frames the monodromy matrices are

$$\begin{pmatrix} e_1' \\ e_2' \\ e_3' \end{pmatrix} = \begin{pmatrix} 1 & 1 & 0 \\ 0 & 1 & 0 \\ 0 & 0 & 1 \end{pmatrix} \begin{pmatrix} e_1 \\ e_2 \\ e_3 \end{pmatrix} \quad \text{and} \quad \begin{pmatrix} f_1' \\ f_2' \\ f_3' \end{pmatrix} = \begin{pmatrix} 1 & -1 & 0 \\ 0 & 1 & 0 \\ 0 & 0 & 1 \end{pmatrix} \begin{pmatrix} f_1 \\ f_2 \\ f_3 \end{pmatrix}, \tag{5}$$

which differ only by the sign of the nondiagonal element. Obviously these two matrices belong to the same conjugacy class of elements of SL(3, Z). Now, if we construct positive rather than negative defect by introducing into the regular lattice the same wedge (as the one in Figure 8) the sign of non diagonal matrix element in the monodromy matrix will change but again by taking two frames which are related one to another by simple rotation over π around e_1 we obtain the same pair of monodromy matrices which differ by the sign of nondiagonal element. Simply this means that the 3D-monodromy matrix cannot distinguish between negative and positive defects.

Naturally, in 3D-lattices we can construct elementary codimension two defects by trivially extending to the third dimension of the 2D-defect introduced for different two-dimensional wedges. There are a lot of possibilities. We restrict ourselves to the three elementary defects, shown schematically in Figure 9. These three defects correspond to removing following wedges from the regular cubic 3D-lattice with coordinates $\{x, y, z\}$ taken along three basis vectors of the lattice:

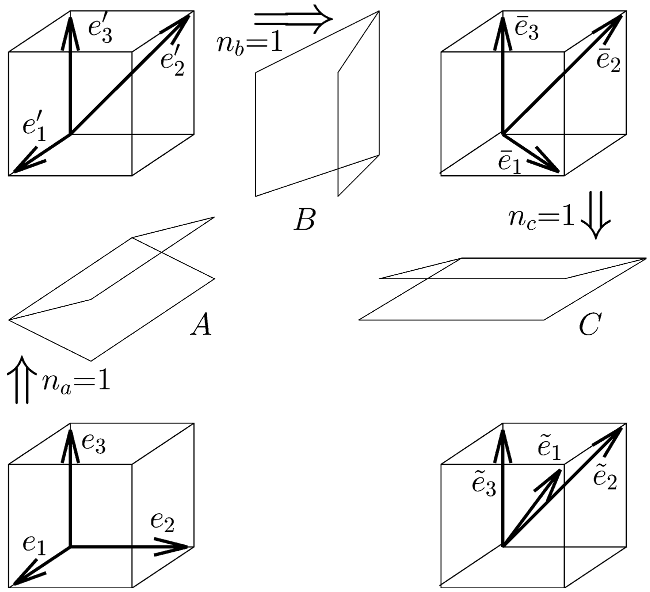

Figure 9. Transformation of 3D-cell along the closed path surrounding three elementary defects, A, B, C, represented by wedges removed from the regular cubic lattice.

(i) The wedge $|z - z_a| < n_a(y - y_a)/2$, corresponding to the negative line defect $\{z = z_a, y = y_a\}$ with amplitude n_a.
(ii) The wedge $|y - y_b| < n_b(x - x_b)/2$, corresponding to the negative line defect $\{y = y_b, x = x_b\}$ with amplitude n_b.
(iii) The wedge $|z - z_c| < n_c(x - x_c)/2$, corresponding to the negative line defect $\{z = z_c, x = x_c c\}$ with amplitude n_c.

We name below these wedges and corresponding defects by letters A, B, and C respectively in order to avoid complicated general notation.

Transformation of the elementary 3D-cell along a closed path surrounding defect A alone and crossing the cut A in direction from negative to positive z values is given by the monodromy matrix

$$\begin{pmatrix} 1 & 0 & 0 \\ 0 & 1 & n_a \\ 0 & 0 & 1 \end{pmatrix}. \tag{6}$$

In the same way the transformation of the elementary 3D-cell along a closed path surrounding defect B alone and crossing the cut B in direction from negative to positive y values is given by the monodromy matrix

$$\begin{pmatrix} 1 & n_b & 0 \\ 0 & 1 & 0 \\ 0 & 0 & 1 \end{pmatrix}. \tag{7}$$

Finally the transformation of the elementary 3D-cell along a closed path surrounding defect C alone and crossing the cut C in direction from positive to negative y values is given by the monodromy matrix

$$\begin{pmatrix} 1 & 0 & n_c \\ 0 & 1 & 0 \\ 0 & 0 & 1 \end{pmatrix}. \tag{8}$$

If now we take the closed path going around all three line defects and crossing cuts A, B, C in the mentioned above way (as shown in Figure 9), the resulting monodromy matrix is the product of three matrices corresponding to elementary defects and has the form

$$\begin{pmatrix} 1 & n_a & n_c \\ 0 & 1 & n_b \\ 0 & 0 & 1 \end{pmatrix}. \tag{9}$$

Figure 9 shows the transformation of the cell (more exactly of the associated frame) for the case when $n_a = n_b = n_c = 1$. Thus it is clear that with three elementary (multiple) cuts we can construct defect which is characterized by arbitrary unipotent matrix in SL(3, Z). In fact, it is known that any element of SL(N, Z) can be represented as a finite product of conjugates of elementary matrices [28, 1]. In particular, any element of SL(3, Z) can be represented as a product of conjugates of at most 60 elementary matrices. This means in our context that it is possible to realize a system of $K \leqslant 60$ elementary monodromy defects which has an arbitrary SL(3, Z) matrix as its global monodromy matrix.

As in 2D-case, the partial classification of defects can be done by their monodromy, taking into account the fact that the monodromy is defined up to conjugation within the group SL(3, Z). If defects are described by monodromy matrices which belong to different classes of conjugated elements of SL(3, Z) group, their defects are different. Nevertheless, it is possible that defects described by monodromy matrices from the same conjugacy class of SL(3, Z) can be distinguished by another invariant. This takes place for positive and negative defects, constructed by adding/removing the same wedge to/from the regular lattice. The monodromy matrix for such pair of 3D-defects belongs to the same class of conjugate elements. We recall that for 2D-case the monodromy matrices for such pair of positive/negative defects belong to different classes of conjugate elements.

We have discussed for 3D-lattice the “integer” monodromy defects, which are of codimension two. In a similar way the fractional defects can be generalized to 3D- (or to N-dimensional) lattices. We note that the fractional monodromy defect always has codimension one.

5. Integrable Classical Singular Fibrations and Monodromy

Now in order to demonstrate the relevance of lattice defects discussed in the previous section to classical monodromy of integrable Hamiltonian systems and to the corresponding lattice of quantum states, we analyze briefly the integrable foliation introduced by Nekhoroshev, Sadovskii, Zhilinskii [23]. The case of $l = 1, k = 1, 2$ has been analyzed in details in [24]. We follow the same approach below in a slightly more general situation.

Let us consider the integrable foliation of four-dimensional phase space $R^4 = \{p_1, q_1, p_2, q_2\}$ defined by two functions F_1, F_2 in involution:

$$F_1 := l\left(\frac{p_1^2}{2} + \frac{q_1^2}{2}\right) - k\left(\frac{p_2^2}{2} + \frac{q_2^2}{2}\right); \tag{10}$$

$$F_2 := \Im\big((q_1 + ip_1)^k (q_2 + ip_2)^l\big) + \left(l\left(\frac{p_1^2}{2} + \frac{q_1^2}{2}\right) + k\left(\frac{p_2^2}{2} + \frac{q_2^2}{2}\right)\right)^s. \tag{11}$$

Here $\Im(X)$ means the imaginary part of expression X. Two functions F_1, F_2 are characterized by three positive integers l, k, s. We suppose that the greatest common divisor of l and $k \geqslant l$ is one and that s is the minimal integer satisfying inequality $s > (l + k)/2$.

We call the map

$$\mathcal{E}\mathcal{M}\colon\ R^4 \to R^2\colon\ (p_1, q_1, p_2, q_2) \to (F_1, F_2) \tag{12}$$

the generalized energy-momentum map. This map defines a singular fibration. The base of this fibration is the plane $R^2 = \{f_1, f_2\}$ of possible values of functions F_1 and F_2. Each fiber Λ_{f_1,f_2} is a common level set of F_1, F_2 functions. Regular fibers of this fibration are two-dimensional tori on which the flow X_{F_1} defines an action of a circle. We are interested in study of this fibration in the neighborhood of its critical value $(0, 0)$. The image of the energy momentum map $\mathcal{E}\mathcal{M}$ in the neighborhood of $(0, 0)$ is shown in Figure 10. The point $(f_1 = 0,\ f_2 = 0)$ is the critical value for integrable fibration (10), (11) for any admissible k and l values including the most trivial case $k = l = 1$ corresponding to the focus-focus singularity with integer monodromy [18, 17, 34, 35]. In the fiber $\Lambda_{0,0}$, the map $\mathcal{E}\mathcal{M}$ has critical point $p_1 = q_1 = p_2 = q_2 = 0$ of rank 0. In the case $l = 1, k > 1$ there is additional line of critical values given by equation $f_2 = f_1^s,\ f_1 < 0$. Each fiber Λ_{f_1,f_2} (which

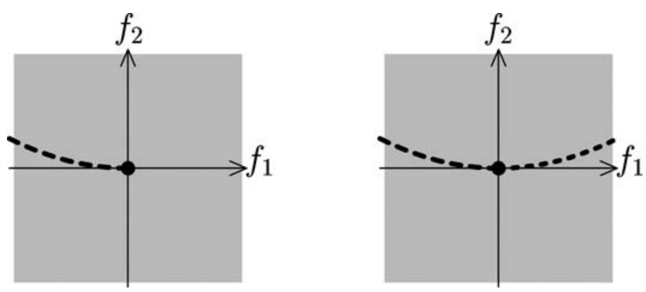

Figure 10. Image of the energy momentum map for integrable fibration F_1, F_2 (10,11) with $l = 1, k > 1$ (left) and $l > 1, k > 1, \gcd(l, k) = 1$ (right).

is a curled torus) corresponding to one of these critical values possesses a circle of critical points of rank 1, corresponding to intersection of a fiber with the plane $p_1 = q_1 = 0$. All these critical points belong to nongeneric trajectory of X_{F_1} whose isotropy group is the cyclic group of order k. In the most general situation of fibration (10), (11) with $k > 1$, $l > 1$, and $\gcd(l, k) = 1$ there are two different strata of critical values: $f_2 = f_1^s$, $f_1 < 0$ and $f_2 = f_1^s$, $f_1 > 0$. Corresponding fibers have critical points of rank 1 lying on trajectories of X_{F_1} with stabilizers being respectively cyclic groups of order k and l.

As soon as fibration is defined we can associate with each regular fiber of this fibration its fundamental group, which is an Abelian group Z^2, and to choose cycles in the fiber which form basis of the fundamental group itself or a basis for a subgroup of finite index. We take a closed trajectory of X_{F_1} as a loop representing one of the basis cycles. To fix another cycle for regular fiber we define the hyperplane σ:

$$\sigma := \sqrt{k}q_2 - \sqrt{l}p_1 \tag{13}$$

and take one of the connected components of intersection $\lambda_{f_1,f_2} = \Lambda_{f_1,f_2} \cap \sigma$ as a loop representing another independent cycle. This is possible except for those regular tori whose intersection with σ is not transversal. The chosen cycles do not form for an arbitrary regular torus the basis of the fundamental group because their intersection number can be different from 1. Nevertheless, they form basis of a subgroup (of finite index) of the fundamental group and this is sufficient for our purposes. This means that globally we have several different charts specifying the choice of basis cycles of certain finite index subgroup of the fundamental group of fibers. We use these charts to calculate the monodromy associated with an arbitrary closed path δ_Γ in R^4 which intersects all fibers transversally. The initial (and final) point of path δ_Γ belongs to regular fiber Λ_{Γ_0} and the path δ_Γ itself can be represented by its projection Γ on the base plane of the fibration. In order to calculate monodromy we look at the evolution of chains representing basic cycles of the initial fiber Λ_{Γ_0} along the path δ_Γ or equivalently along its projection Γ on the plane (f_1, f_2).

In the presence of one-dimensional singular strata on the image of energy-momentum map (see Figure 10) it is important to define the class of chains which can be deformed continuously through the singular stratum. Such chains are called passable and for each singular stratum there is a subgroup of passable chains [24]. The continuous deformation of passable chains between different charts can result in a discontinuous modification of their expression in terms of basis cycles when passing from one chart to another. We can choose at the initial point $\Gamma_0 = \{f_1 = 0, f_2 < 0\}$ of the contour Γ the chain corresponding to one connected component of the intersection line. In order to deform this chain through the tori whose intersection with σ is not transversal we need to replace it by a homotopically equivalent chain which avoids the branching points of the intersection locus. This program was realized in [24] in the case of $l = 1$, $k = 1, 2$. The key point is the description of intersection locus $\Lambda_{f_1,f_2} \cap \sigma = \lambda_{f_1,f_2}$ in the case $f_1 = 0$ for small positive and small negative f_2 values. We call the corresponding curves $\lambda_{f_1,f_2}|_{f_1=0}$ skeleton curves. Deformation of intersection locus along the contour Γ and the associated transformation of chains chosen to represent basic cycles for the Γ_0 regular torus can be understood easier if we analyze them in parallel in σ and on the Λ_{f_1,f_2} torus using standard representation of torus as a rectangle with properly identified sides.

The description and analysis of intersection locus λ_{f_1,f_2} becomes more transparent if we use proper coordinates. Namely in σ we introduce coordinates (x, y, p_1) with

$$x = \sqrt{l/2}q_1 - \sqrt{k/2}p_2; \qquad y = \sqrt{l/2}q_1 + \sqrt{k/2}p_2. \tag{14}$$

In these coordinates the function F_1 has the extremely simple form

$$F_1 = xy. \tag{15}$$

This means that for $f_1 > 0$ the components of the intersection locus lie in σ on two-sheet hyperboloid surface situated in first and third quadrants. In the case of $f_1 < 0$ the components of the intersection locus in σ belong to the hyperboloid surface situated in second and fourth quadrants. Finally for $f_1 = 0$ the two-sheet hyperboloid degenerates into two intersecting planes $x = 0$ and $y = 0$ which contain the skeleton curves. Typically the skeleton curve consists of several disconnected components which are planar curves lying in either $x = 0$ or in $y = 0$ planes, or are the union of planar curves.

In the case of $f_2 > 0$ the skeleton curve for $f_1 = 0$ consists of two planar components which belong to $x = 0$ and $y = 0$ planes and have two common points. For $f_1 = 0+$ and for $f_1 = 0-$ this branched curve splits into two connected components which lie in 1-st and 3-rd quadrants for $f_1 = 0+$ and in 2-nd and 4-th quadrants for $f_1 = 0-$. Number of components and number of branching points do not depend on k and l in the case of $f_2 > 0$.

In the case of $f_2 < 0$ the number of connected components of intersection line and the number of branching points depend on k and l. We describe in Table I the situation in the case of fibration (10), (11) with $l = 1$ and arbitrary k.

The skeleton curves for $1 : (-k)$ resonance with $k = 2, 3, 4$ are shown in Figures 11, 12, and 13. To reconstruct the representation of the intersection locus on the torus we look at trajectories of X_{F_1} and analyze their intersection with σ which obviously belongs to λ_{f_1,f_2} as well. In order to choose the reference point on the intersection locus λ_{Γ_0} we start at $t = 0$, say, at point lying on one of connected components of the intersection locus at $x = y = 0$. This trajectory crosses further the intersection locus at time satisfying the equation

$$\sin(t) + \sin(kt) = 0. \tag{16}$$

The solutions $t = 2s\pi/(k + 1)$, and $t = (2s + 1)\pi/(k - 1)$, with s-integer, give immediately the order in which the trajectories of X_{F_1} cross the (components of the) intersection locus. Points of crossing are denoted consecutively by

Table I. Numbers of connected components of intersection line $\Lambda_{f_1,f_2} \cap \sigma$ in the case of $f_2 < 0$ for $1:(-k)$ resonance. Second column gives the numbers of components lying in 2-nd and 4-th quadrant for negative f_1 values. Third column gives the numbers of components lying in $y = 0$ and $x = 0$ planes together with the number of branching points, n_{br}. Fourth column gives the numbers of components lying in 1-st and 3-rd quadrant for positive f_1 values.

k	$f_1 = 0-$		$f_1 = 0$			$f_1 = 0+$	
	2-nd	4-th	λ^x	n_{br}	λ^y	1-st	3-rd
0 mod 4	k	k	$k+1$	0	$k-1$	$k+1$	$k-1$
1 mod 4	k	k	$k+1$	0	$k-1$	k	k
2 mod 4	k	k	$k+1$	0	$k-1$	$k-1$	$k+1$
3 mod 4	k	k	$k+1$	4	$k-1$	k	k

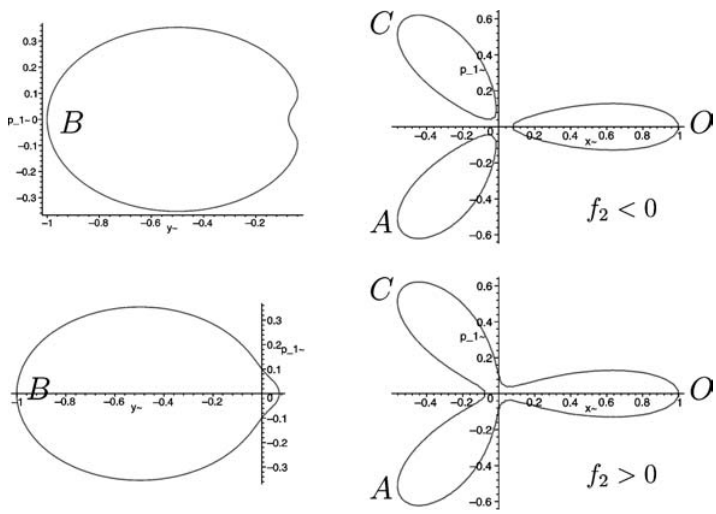

Figure 11. $1:(-2)$ case. λ^x_{0,f_2} and λ^y_{0,f_2} components of intersection locus for small negative and positive values of f_2.

letters O, A, B, C in Figure 11 and by A, B, ... in Figures 12, 13. Specific notation for $1:(-2)$ case is chosen to be in accordance with the notation used in [24]. Relative orientation of different components of the intersection locus is chosen in such a way that it takes into account the sign of the height function induced on tori by hyperplane σ.

Evolution of the intersection locus along the contour Γ is represented schematically on the torus in Figures 14, 15, and 16 for model problems with $1:(-2)$, $1:(-3)$, and $1:(-4)$ resonances respectively.

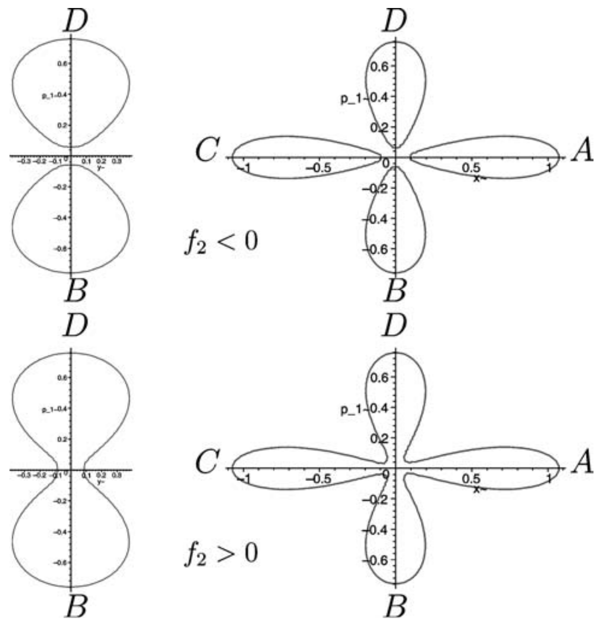

Figure 12. 1 : (−3) case. λ^x_{0,f_2} and λ^y_{0,f_2} components of intersection locus for small negative and positive values of f_2.

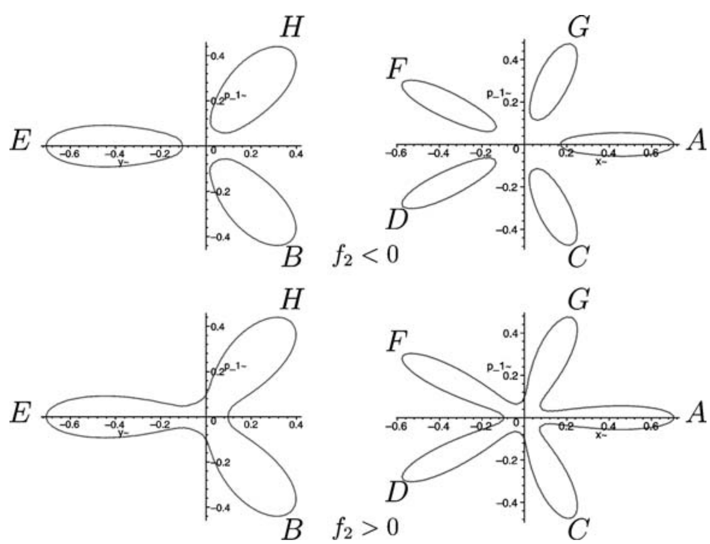

Figure 13. 1 : (−4) case. λ^x_{0,f_2} and λ^y_{0,f_2} components of intersection locus for small negative and positive values of f_2.

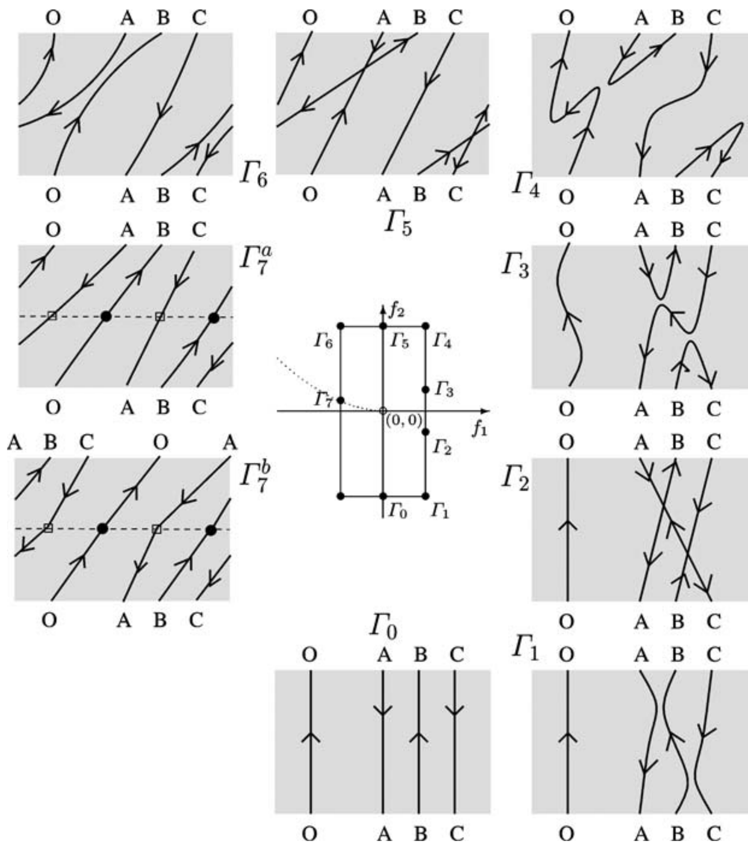

Figure 14. Evolution of the intersection locus $\Lambda_{f_1,f_2} \cap \sigma$ along the contour Γ represented on the torus maps. The case of $1:(-2)$ resonance model. Two representations of singular 2-curled torus are given (points Γ_7^a and Γ_7^b).

Without entering into details we just formulate here the most important results which can be stated on the basis of detailed analysis of these model cases.

(i) Models with $k = 3 \bmod 4$ should be studied separately due to specific behavior of skeleton curves for $f_2 < 0$. All other cases are quite similar although the number of nonregular points on the contour Γ increases as k increases.

(ii) Crossing 1D-singular stratum is responsible for the fact that only chains representing cycles of a subgroup of index k of the fundamental group are passable [24]. We recall that in the case of $l:(-k)$ models there are two 1D-strata each of which impose their own restriction on the type of subgroup to be considered.

(iii) Construction of the deformation of passable chains through the fiber $\Lambda_{f_1,f_2}|_{f_1=0,f_2>0}$ fiber is the most important step in monodromy calculation. This deformation can be done by replacing the chain formed at $f_1 = 0+$ by the intersection locus by a homotopically equivalent chain which is formed by fragments of inter-

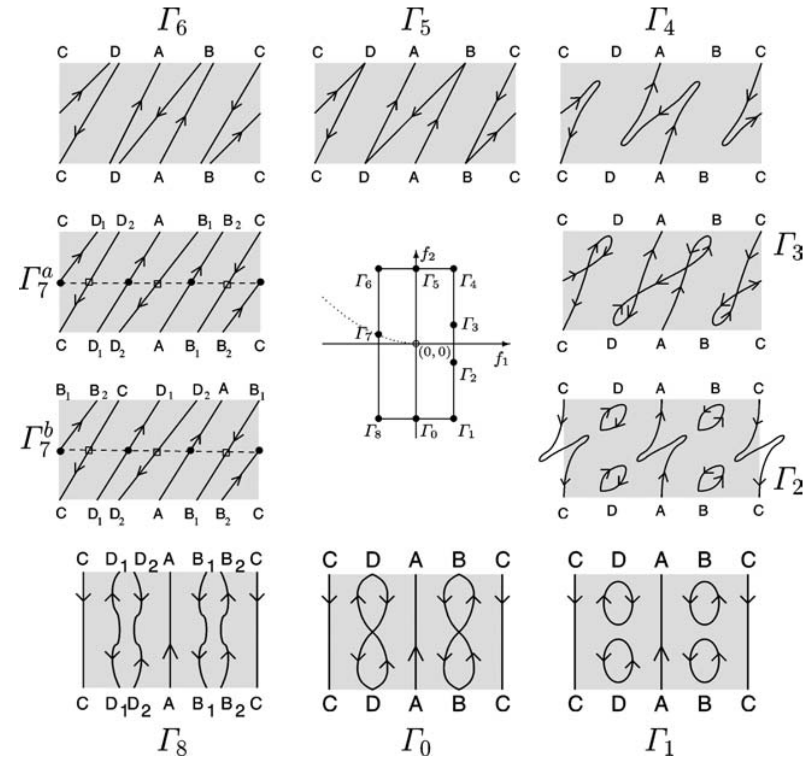

Figure 15. Evolution of the intersection locus $\Lambda_{f_1,f_2} \cap \sigma$ along the contour Γ represented on the torus maps. The case of $1:(-3)$ resonance model. Two representations of singular 3-curled torus are given (points Γ_7^a and Γ_7^b).

section locus (preserving their orientation) and trajectories of the field X_{F_1} which do not belong to σ. The so formed equivalent chain can be deformed smoothly through the $\Lambda_{f_1,f_2}|_{f_1=0,f_2>0}$ fiber because it does not contain branch points of the intersection locus. In all cases the chain initially chosen at point Γ_0 as a proper multiple of one of connected components of intersection locus becomes after crossing the $\Lambda_{f_1,f_2}|_{f_1=0,f_2>0}$ fiber the chain represented as a linear combination of one component of the intersection locus and a properly oriented trajectory of the system with Hamiltonian F_1.

If we choose as the basis of cycles at the initial point Γ_0 the cycle γ represented by trajectories of X_{F_1} and cycle γ_0 represented by one of the components of intersection locus $\Lambda_{\Gamma_0} \cap \sigma$, the deformation of the chain chosen as a k-multiple of one component of the intersection locus leads to a chain representing the $k\gamma_0 - \gamma$ cycle after going in a counterclockwise direction along contour Γ. Taking into account the fact that the trajectory of X_{F_1} always represent the same cycle we get the transformation of basic cycles of the Λ_{Γ_0} fiber

$$\gamma \longrightarrow \gamma; \qquad k\gamma_0 \longrightarrow k\gamma_0 - \gamma, \tag{17}$$

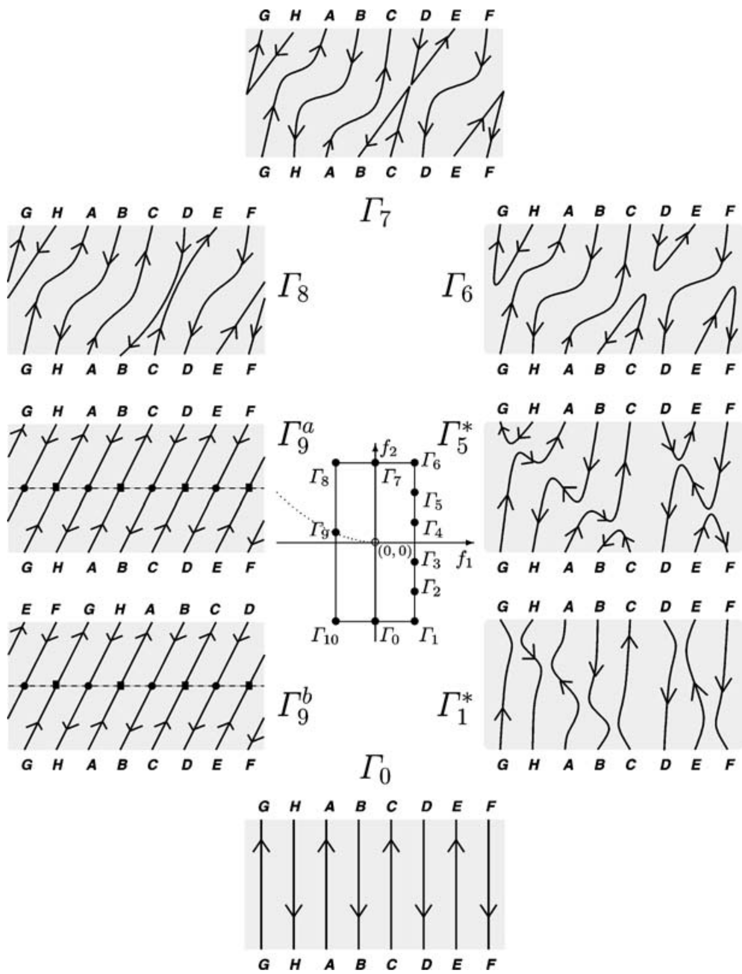

Figure 16. Schematic evolution of the intersection locus $\Lambda_{f_1,f_2} \cap \sigma$ along the contour Γ represented on the torus maps. The case of $1:(-4)$ resonance model. Two representations of singular 4-curled torus are given (points Γ_9^a and Γ_9^b).

which can easily be written in the form of monodromy matrix with fractional coefficients after returning back to the initial cycles γ, γ_0.

We comment now briefly the figures illustrating the behavior of classical dynamical systems for $1:(-k)$ cases ($k = 2, 3, 4$).

In the case of $k = 2$ (see Figures 11, 14) there are 4 connected components of intersection at Γ_0 point of the contour Γ. We choose the chain $2(O\,O)$ representing the double cycle γ_0. This chain represents the same cycle along the contour Γ if the point Γ_5 is not crossed. At the same time three other components form one connected component crossing point Γ_2 associated with the singularity of the intersection locus. In the neighborhood of Γ_5 point the chain $2(OO)$ is replaced by a homotopically equivalent chain which can be deformed smoothly through the point Γ_5 to chain $OBO-\gamma$. Further deformation of the chain $OBO-\gamma$ is smooth except at the point Γ_7 corresponding to singular stratum. At this point of the contour Γ the fragment OBO forms a figure eight and splits into two components OO and BB. Further deformation along the contour Γ till the point Γ_0 brings the initial chain $2(OO)$ to the chain $(OO)+(BB)-\gamma$ which is equivalent to the chain $2(OO)-\gamma$ representing the cycle $2\gamma_0-\gamma$. Thus we associate with the contour Γ the transformation of the cycles of the index 2 subgroup of the fundamental group of Λ_{Γ_0} given by (17) with $k=2$. This is exactly the monodromy transformation for fractional $1:2$ defect of quantum state lattice.

The case of $1:(-3)$ resonance integrable model (see Figures 12, 15) has important difference because at Γ_0 the intersection locus $\Lambda_{\Gamma_0}\cap\sigma$ has four branching points. Nevertheless we can take as a passable chain the triple loop $3(AA)$. We need to use triple loop in order to pass continuously the singular stratum (i.e. point Γ_7 on the contour Γ) (Figure 15). The deformation of the chain $3(AA)$ along Γ does not change its homotopy type even when passing the point Γ_3 where the fusion of loops A, B, D takes place. When approaching the point Γ_5 (for example at point Γ_4) we have chain $3(AA)$ which should be replaced by a homotopy equivalent chain in order to avoid the singularity at point Γ_5 which is due to formation of two common points on two connected components of the intersection locus belonging at $f_1\neq 0$ to two different sheets of the hyperboloid $xy=f_1$. Passing through the point Γ_5 transforms $3(AA)$ chain into the linear combination $(ABDA)-\gamma$. Again the fragment $(ABDA)$ splits into three loops $(AA)+(B_2B_2)+(D_1D_1)$ when passing through the singular stratum (point Γ_7 in Figure 15). This means that at point Γ_8 the initial chain $3(AA)$ becomes the chain $(AA)+(B_2B_2)+(D_1D_1)-\gamma$ formed by trajectory of X_{F_1} and three homotopy equivalent loops which can equally be represented as $3(AA)$. Final deformation till Γ_0 gives again the transformation of chains $3(AA)\rightarrow 3(AA)-\gamma$ corresponding to transformation of cycles of an index 3 subgroup of the fundamental group (17) and to the monodromy of the $1:3$ fractional defect.

The situation in the case of $1:(-4)$ resonance integrable model (see Figures 13, 16) is quite similar to the $1:(-2)$ case. The only difference is the larger number of connected components of the intersection locus and the larger number of points on the contour Γ corresponding to fusion of different components. We can take again as passable chain at the initial point Γ_0 the multiple (quadruple) loop $4(AA)$. Between points Γ_1 and Γ_6 (Figure 16) 8 initial components of intersection locus rearrange into two connected components. Multiple of one of them, namely $4(ACBHGA)$ is homotopy equivalent to the initial multiple loop $4(AA)$. Crossing Γ_7 point is done by replacing the $4(ACBHGA)$ chain by a homotopy equivalent one which becomes at point Γ_8 the chain $(ACEGA)-\gamma$. Passing point Γ_9 the fragment $(ACEGA)$ splits into four homotopy equivalent loops $(AA)+(CC)+(EE)+(GG)$ and the final chain at point Γ_0 can be again replaced by combination $4(AA) - \gamma$ which corresponds to (17) for $k = 4$ and coincides with monodromy for $1:4$ fractional defect of quantum state lattice.

Demonstration of the cycle deformation was only outlined here. The main idea of this analysis was to show the quite simple and useful interpretation of monodromy of classical integrable fibration in terms of defects of regular lattices. In turn this can be considered as a typical qualitative feature of the joint quantum spectrum of several commuting observables due to simple interpretation of the quantum state lattice as points of associated classical Hamiltonian system having integer values of its action variables. In the next section we try to explain why the study of these qualitative features is interesting from the physical point of view, namely from the point of view of intra-molecular dynamics and spectra.

6. Molecular Examples

Recent interest in study of Hamiltonian monodromy in classical systems and of its manifestation in corresponding quantum systems was due to the discovery by physicists of a qualitative effects in simple molecular model systems and in real molecular spectra which turn out to be directly related to Hamiltonian monodromy. We summarize here the main results and systems studied up to now together with remaining open problems.

The first concrete example of a simple system with monodromy was the spherical pendulum [4] studied in classical and quantum mechanics [5]. These works inspired further analysis of the standard problem in atomic and molecular physics of angular momentum coupling from the point of view of monodromy [27, 15]. The discovery of characteristic qualitative features of patterns of quantum states of the hydrogen atom in external fields and their explanation in terms of monodromy for an integrable approximation [7] was the most important step in proving the physical interest of monodromy. Further studies of such molecular problems as H_2^+ [30], H_2O [2], LiCN [16] confirm the presence of integer monodromy in concrete molecular problems and its easily visualized interpretation as a lattice defect. The next important step in the application of monodromy was the demonstration of existence of integer monodromy in the integrable approximation describing the pattern of quantum states of CO_2 molecule taking into account the $1:1:2$ resonance between stretching and doubly degenerate bending vibrations [6, 14]. This particular model of nonlinear $1:1:2$ resonance oscillators has many important applications in fluid and plasma systems and in laser-matter interaction. The manifestation of monodromy effects in these latter areas remains an open question. Fractional monodromy [23] has not yet been found in molecular models. Nevertheless the mathematical analysis has been done for models which correspond to several nonlinear coupled oscillators in resonance. This situation is typical in molecular problems where resonances are clearly seen in the quantum spectrum through the appearance of the so-called vibrational polyads [26]. The specific pattern of quantum states related to the presence of a codimension one "fractional defect" [3] is much easy to detect than monodromy itself.

In all of the cases discussed above the understanding of the presence of monodromy is of crucial importance for interpretation and assignment of molecular spectra which is traditionally based on local analysis of regular behavior of quantum states and related physical quantities. The presence of monodromy explains the absence of global (even approximate) action-angle variables in classical problems [22, 10] and the absence of a global system of quantum numbers for corresponding quantum problem [11]. We expect that the presence of monodromy is highly important as well for description of molecular excitation processes and chemical reactions. The search for elementary chemical reactions controlled by the dynamical features related to monodromy now seems to be the most challenging problem from the point of view of molecular applications of monodromy.

7. Conclusions

The comparative analysis of quantum lattice defects and singularities of classical integrable fibrations shows that "codimension two" integer monodromy defects and "codimension one" fractional monodromy defects can be considered as models describing the qualitative features of joint spectrum of several commuting observables [33, 32]. Up to now the qualitative behavior of the joint spectrum itself has been mainly studied. It is more or less evident that certain qualitative features related to monodromy should be present when quantum wave functions of corresponding quantum states are analyzed.

Extension of the qualitative analysis of patterns of quantum states for problems with monodromy to quantum wave-functions and in particular to dynamical processes induced by the interaction with external fields seems to be one of priority directions for further physical applications.

The analysis of classical and quantum problems with monodromy realized till now deals with cases when monodromy is associated with the closed path which belongs everywhere to one fiber of the integrable fibration. Such restriction seems to be too strong for many real molecular examples. It would be interesting to generalize the qualitative description to the cases when a closed path crosses points where fusion of different connected components of the inverse image of the energy-momentum map takes place. This step requires further generalization of the admissible paths and of the notion of monodromy itself.

Another important generalization is the analysis of the possible existence of dynamical analogs of defects of regular lattices of higher codimension and more detailed correspondence between lattice defects [19, 20] and qualitative features of dynamical systems (classical or quantum) which is absent up to now.

The relation between quantum monodromy and the phenomenon of redistribution of quantum states between branches in the energy spectrum was observed on several occasions [27, 12, 13] in the context of study of the same problem in pure quantum, semi-quantum, and purely classical approaches. A mathematically rigorous interpretation of such relation is still lacking.

Acknowledgements

Author thanks Drs. R. Cushman, K. Efstathiou, A. Giacobbe, V. Matveev, N. Nekhorochev, D. Sadovskii, S. Vũ Ngọc for valuable discussions and comments. This work was supported by EU project *Mechanics And Symmetry In Europe (MASIE)*, contract HPRN-CT-2000-00113.

References

1. Carter, D. and Keller, G.: Bounded elementary generation of $SL_n(\mathcal{O})$, *Amer. J. Math.* **105** (1983), 673–687.
2. Child, M. S., Weston, T. and Tennyson, J.: Quantum monodromy in the spectrum of H_2O and other systems, *Mol. Phys.* **96** (1999), 371–379.
3. Colin de Verdier, Y. and Vũ Ngọc, S.: Singular Bohr–Sommerfeld rules for 2D integrable systems, *Ann. Ec. Norm. Sup.* **36** (2003), 1–55.
4. Cushman, R. H. and Bates, L. M.: *Global Aspects of Classical Integrable Systems*, Birkhäuser, Basel, 1997.
5. Cushman, R. H. and Duistermaat, J. J.: The quantum mechanical spherical pendulum, *Bull. Amer. Math. Soc.* **19** (1988), 475–479.
6. Cushman, R. H., Dullin, H. R., Giacobbe, A., Holm, D. D., Joyeux, M., Lynch, P., Sadovskii, D. A. and Zhilinskii, B. I.: The CO_2 molecule as a quantum realization of the 1:1:2 resonant swing-spring with monodromy, *Phys. Rev. Lett.* **93** (2004), 024302-1-4.
7. Cushman, R. H. and Sadovskií, D. A.: Monodromy in the hydrogen atom in crossed fields, *Physica D* **142** (2000), 166–196.
8. Cushman, R. H. and Vũ Ngọc, S.: Sign of the monodromy for Liouville integrable systems, *Ann. Inst. H. Poincaré* **3** (2002), 883–894.
9. Cushman, R. H. and Zhilinskii, B.: Monodromy of a two degrees of freedom Liouville integrable system with many focus–focus singular points, *J. Phys. A: Math. Gen* **35** (2002), L415–L419.
10. Duistermaat, J. J.: On global action angle coordinates, *Comm. Pure Appl. Math.* **33** (1980), 687–706.
11. Efstathiou, K., Joyeux, M. and Sadovskii, D. A.: Global bending quantum numbers and the absence of monodromy in the HCN$\leftrightarrow$CNH molecule, *Phys. Rev. A* **69**(3) (2004), 032504-1-15.
12. Faure, F. and Zhilinskií, B. I.: Topological Chern indices in molecular spectra, *Phys. Rev. Lett.* **85** (2000), 960–963.
13. Faure, F. and Zhilinskií, B. I.: Topologically coupled energy bands in molecules, *Phys. Lett. A* **302** (2002), 242–252.
14. Giacobbe, A., Cushman, R. H., Sadovskii, D. A. and Zhilinskii, B. I.: Monodromy of the quantum 1:1:2 resonant swing spring, *J. Math. Phys.* **45** (2004), 5076–5100.
15. Grondin, L., Sadovskií, D. A. and Zhilinskií, B. I.: Monodromy in systems with coupled angular momenta and rearrangement of bands in quantum spectra, *Phys. Rev. A* **65** (2002), 012105-1-15.
16. Joyeux, M., Sadovski, D. A. and Tennyson, J.: Monodromy of the LiNC/NCLi molecule, *Chem. Phys. Lett.* **382**(3–4) (2003), 439–442.

17. Lerman, L. M. and Umanskií, Ya. L.: *Four Dimensional Integrable Hamiltonian Systems with Simple Singular Points*, Transl. Math. Monographs 176, Amer. Math. Soc., Providence, RI, 1998.
18. Matveev, V. S.: Integrable Hamiltonian systems with two degrees of freedom. The topological structure of saturated neighborhoods of points of focus–focus and saddle–saddle type, *Sb. Math.* **187**(4) (1996), 495–524.
19. Mermin, N. D.: The topological theory of defects in ordered media, *Rev. Modern Phys.* **51** (1979), 591–648.
20. Michel, L.: Symmetry defects and broken symmetry. Configurations. Hidden symmetry, *Rev. Modern Phys.* **52** (1980), 617–651.
21. Michel, L. and Zhilinskii, B.: Symmetry, invariants, topology. I. Basic tools, *Phys. Rep.* **341** (2001), 11–84.
22. Nek͡horoshev, N. N.: Action-angle variables and their generalizations, *Trans. Moscow Math. Soc.* **26** (1972), 180–198.
23. Nekhoroshev, N. N., Sadovskii, D. A. and Zhilinskii, B. I.: Fractional monodromy of resonant classical and quantum oscillators, *C. R. Acad. Sci. Paris, Ser. I* **335** (2002), 985–988.
24. Nekhoroshev, N. N., Sadovskii, D. A. and Zhilinskii, B. I.: Fractional monodromy, in preparation.
25. Rankin, R. A.: *Modular Forms and Functions*, Cambridge Univ. Press, Cambridge, 1977, Ch. 1.
26. Sadovski, D. A. and Zhilinski, B. I.: Counting levels within vibrational polyads. Generating function approach, *J. Chem. Phys.* **103** (1995), 10520–10536.
27. Sadovskií, D. A. and Zhilinskií, B. I.: Monodromy, diabolic points, and angular momentum coupling, *Phys. Lett. A* **256** (1999), 235–244.
28. Soulé, C.: An introduction to arithmetic groups, arXiv:math.GR/0403390.
29. Stanley, R. P.: *Enumerative Combinatorics*, Wadsworth & Brooks/Cole, Montrey, CA, 1986; Vol. 1, Chapter 4.4.
30. Waalkens, H., Junge, A. and Dullin, H. R.: Quantum monodromy in the two-center problem, *J. Phys. A: Math. Gen.* **36** (2003), L307–L314.
31. Zhilinskií, B. I.: Symmetry, invariants, and topology in molecular models, *Phys. Rep.* **341** (2001), 85–171.
32. Zhilinskií, B. I.: Reorganization of energy bands in quantum finite particle systems, In: *Group 24: Physical and Mathematical Aspects of Symmetries*, IOP Conference Series 173, Institute of Physics Publishing, Bristol, 2002, pp. 625–628.
33. Zhilinskií, B. I.: Hamiltonian monodromy as lattice defect, arXiv:quant-ph/0303181, 2003.
34. Zung, N. T.: A note on focus–focus singularities, *Differential Geom. Appl.* **7** (1997), 123–130.
35. Zung, N. T.: Another note on focus–focus singularities, *Lett. Math. Phys.* **60** (2002), 87–99.